

# DistillAdapt: Source-Free Active Visual Domain Adaptation

Divya Kothandaraman\*, Sumit Shekhar\*\*, Abhilasha Sancheti\*\*, Manoj Ghuhana\*\*, Tripti Shukla\*\*, Dinesh Manocha\*

\* University of Maryland College Park, \*\* Adobe Research

**Abstract.** We present a novel method, DistillAdapt, for the challenging problem of Source-free Active Domain Adaptation (SF-ADA). The problem requires adapting a pre-trained “source” domain network to a “target” domain, within a provided budget for acquiring labels in the “target” domain, while assuming that the source data is not available for adaptation, due to privacy concerns or otherwise. DistillAdapt is one of the first approaches for SF-ADA, and holistically addresses the challenges of SF-ADA via a novel Guided Attention Transfer Network (GATN) and an active learning function,  $H_{AL}$ . The GATN enables selective distillation of features from the pre-trained network to the target network using a small subset of annotated target samples mined by  $H_{AL}$ .  $H_{AL}$  acquires samples at batch-level and balances transfer-ability from the pre-trained network and uncertainty of the target network. DistillAdapt is task-agnostic, and can be applied across visual tasks such as classification, segmentation and detection. Moreover, DistillAdapt can handle shifts in output label space. We conduct experiments and extensive ablation studies across 3 visual tasks, *viz.* digits classification (MNIST, SVHN), synthetic (GTA5) to real (CityScapes) image segmentation, and document layout detection (PubLayNet to DSSE). We show that our source-free approach, DistillAdapt, results in an improvement of 0.5% – 31.3% (across datasets and tasks) over prior adaptation methods that assume access to large amounts of annotated source data for adaptation.

## 1 Introduction

Deep learning solutions for visual applications such as semantic segmentation [56,53], image classification, and document layout analysis [24,44] require a large amount of annotated data. Hence, the recent trend has been to re-use models pre-trained on large datasets and fine tune on a small set of labeled task-specific data. Active Learning (AL) [2,39,48,45] is typically used to sample and annotate within a fixed budget (*e.g.* 5% of the available corpus of unlabeled data [10]) to maximize the models’ performance. Typical active learning strategies include modelling diversity and uncertainty for efficient sampling [10,4].

However, in real world cases, the “target” domain, where the learnt model is being deployed, can have a different distribution than the “source” domain

where it is pre-trained on. The ubiquitous problem of the distribution of the target domain being different from the source domain can be solved by domain adaptation. Prior work on Active Domain Adaptation (ADA) [4,52,39] has explored the use of annotated “source”-data from a related domain to transfer knowledge (via domain adaptation) to the new “target”-domain dataset, within a fixed budget of annotating the “target” data. The biggest drawback of ADA is that it requires a large amount of annotated source data. This is prohibitive in scenarios like autonomous driving where the system only has access to a network *pre-trained* on the source data. The source data itself is **unavailable** after the pre-training, due to privacy issues or storage constraints [22,23].

In this work, we focus on the challenging problem of Source-free Active Domain Adaptation, SF-ADA, where we have access to a pre-trained “source” network, but the source data is not available due to privacy concerns or otherwise. Further, an unlabeled target dataset, and a small budget for acquiring labels in the target domain is specified. To the best of our knowledge, this is the first approach towards SF-ADA. Previous approaches on source-free adaptation (SFDA) [26,58] are task-specific and do not investigate performance improvement through active learning. We believe that an effective solution for SF-ADA should exploit the complementarity of SFDA and AL. The AL algorithm should choose samples that facilitate *knowledge transfer* dictated by the adaptation method. By the same token, the adaptation method needs to learn features that help the AL strategy *mine effective samples*. Thus, an effective SF-ADA approach needs to holistically model AL and adaptation.

### 1.1 Main Contributions:

We present DistillAdapt, one of the first approaches for Source-Free Active Domain Adaptation (SF-ADA). DistillAdapt holistically addresses two key challenges of SF-ADA via two complementary components: the Guided Attention Transfer Network (GATN) and an active learning algorithm,  $H_{AL}$ :

- *Knowledge transfer*: GATN transfers relevant knowledge at the feature level from the pre-trained network to the target network (Figure 1). GATN uses a transformation network to modulate the features of the pre-trained network followed by guided attention for selective distillation to the target network. The target network guides the knowledge transfer via labeled samples selected through AL.
- *Mining samples*: The effectiveness of GATN depends on the fixed budget of samples mined from the target dataset. While it is important to choose samples that are similar to the distribution familiar to the pre-trained network, we need to ensure that the chosen samples are informative to the network w.r.t. the target dataset.  $H_{AL}$  fuses transferability from the pre-trained network, as well as uncertainty w.r.t. the target network.

DistillAdapt has multiple benefits. Knowledge transfer happens at the feature space (output of the network before the decoder). Thus, our architecture is label

space-agnostic and can handle domains that contain different number and types of classes. Our method is task-agnostic, and can be applied across various visual tasks. The source model is not required while testing and can be discarded after training.

We evaluate our approach across three tasks, to highlight the effectiveness of DistillAdapt. On classification datasets (MNIST, SVHN), we demonstrate that even without the source data, DistillAdapt performs similar to or better than the prior active domain adaptation methods [52,39] that use annotated source data. Next, we evaluate on MNIST under 2 distinct cases of shift in output label space and show that DistillAdapt is able to achieve 99.4% of the accuracy in case of no shift in the label space, thus establishing the effectiveness of our model in scenarios with label shift. Our experiments on the CityScapes dataset for semantic segmentation improves accuracy by 5.57% over fine-tuning. We also highlight the benefits of SF-ADA over other adaptation paradigms in Table 7. Finally, we conduct experiments on adaptation for document layout detection from PubLayNet to DSSE, where there is a shift in the output label space. DistillAdapt imparts a relative improvement of 31.3% over fine-tuning of the target network on the small dataset.

## 2 DistillAdapt

For Source-Free Active Domain Adaptation (SF-ADA), we assume (i) a network,  $N_S$ , pre-trained on a source-domain,  $S$  (the source data is not available for adaptation) and (ii) an unlabeled target domain  $T$  from which we are allowed to annotate  $B$  images. The goal is to mine  $B$  images to facilitate adaptation from  $N_S$  to a network,  $N_T$  which learns robust task-specific features for the target domain.

We postulate that methods designed for SF-ADA need to address two facets: (i) Effective knowledge transfer from the pre-trained network to the target network using the small set of annotated samples mined, as well as to help sample mining in the next step and (ii) Intelligently choose samples to annotate, to facilitate knowledge transfer as well as span the spectrum of samples contained in the target dataset. Consequently, our proposed solution for SF-ADA, DistillAdapt (Figure 1), consists of two complementary components: (i) Guided Attention Transfer Network (GATN) for knowledge transfer (ii) an active learning strategy,  $H_{AL}$ , for acquiring samples. The goal of the AL strategy is to sample images that are important for the target network and transfer well from the pre-trained network (without any negative transfer), while GATN strives to learn robust target domain feature maps. DistillAdapt is a generic approach that can be applied across various visual tasks (classification, detection, segmentation). Moreover, it can handle shifts in label space from the source to the target domain where the source and target domains may not have the same set of classes. We now describe our method in detail.

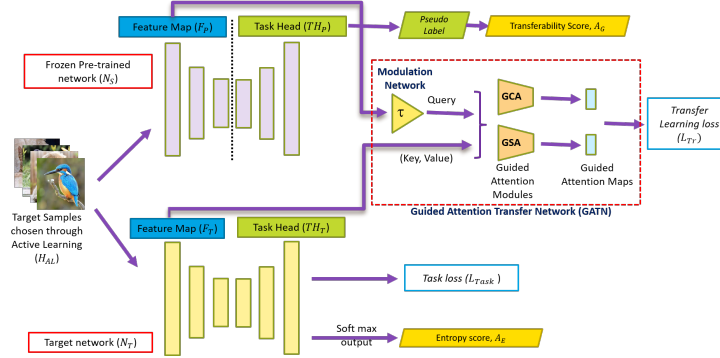


Fig. 1: We present a novel method, **DistillAdapt**, for **Source Free Active Domain Adaptation**. DistillAdapt consists of two key components: Guided Attention Transfer Network (GATN) and an active learning strategy  $H_{AL}$ .

## 2.1 Method Description

Prior work on SFDA [23,30] has relied on alignment between source and target data to guide the adaptation process. This requires the system to emulate source-data in a source-free setting which does not generalize across complex tasks [30,20]. Instead, we adopt a novel distillation-based transfer learning strategy at feature level. The selective distillation, combined with AL strategy  $H_{AL}$ , enables domain-specific learning for target network using chosen samples, while relevant domain-agnostic knowledge is retained from the pre-trained source network via attentive distillation.

For initiating the distillation, the frozen pre-trained network,  $N_S$  is split into feature map network  $F_P$  followed by the frozen task head  $TH_P$ . Concurrently, the target network,  $N_T$  is used to generate target feature map  $F_T$  and a trainable task head  $TH_T$ .  $F_P$  and  $F_T$  are passed through the Guided Attention Transfer Network (GATN), which constrains the target network via a transfer learning loss  $L_{Tr}$ . Our use of guided attention enables the target network to retain the domain-agnostic features from the pretrained network. The GATN, as well as the pre-trained network, can be discarded after training, i.e. they are not required in the evaluation phase. The GATN consists of a modulation network,  $\tau$ , for perturbing  $F_P$  to avoid trivial solutions. The transformed  $F_P$  and  $F_T$  are then fed to two guided attention modules. The guided attention modules consist of Guided Spatial Attention (GSA) and Guided Channel Attention (GCA) [60,11] to compute attention across spatial and channel dimensions respectively. The overall adaptation framework (GATN and the target network) is jointly trained with a combination of the transfer learning loss  $L_{Tr}$  and the task specific loss  $L_{task}$ .

The GATN is complemented with a robust sampling with the active learning strategy,  $H_{AL}$ . Samples are chosen such that they facilitate transfer learning and trade-off uncertainty for the target network, an indicator of informativeness w.r.t.

the target domain [39]. We train the target network through mining samples from the target domain dataset in mini-batches using  $H_{AL}$  until the desired budget  $B$  is achieved. The steps in the training routine are as follows:

- Initialize target network with parameters of the pre-trained source network
- Perform the following steps until the total number of samples mined from the target dataset does not exceed  $B$ .
  - Use the AL strategy  $H_{AL}$ , the pre-trained network and the target network trained in the previous iteration, to mine samples from the target dataset. Accumulate in the set of samples that have already been mined, and annotate them. This gives us a labeled target subset  $T_L$  and an unlabeled target subset  $T_{UL}$ .
  - Jointly train the target network and GATN using  $T_L$  and  $T_{UL}$  by the application of  $L_{task}$  and  $L_{Tr}$ .

## 2.2 Guided Attention Transfer Network (GATN)

In this section, we describe the Guided Attention Transfer Network (GATN) in details. We first compute feature maps from the pre-trained network  $F_P$  and the target network  $F_T$  for the target dataset input sample  $I$ . The pre-trained network feature map  $F_P$  is transformed using a four-layer fully convolution network  $\tau$ , to output  $F_{P-tr}$ . This along with  $F_T$  are then passed to spatial guided attention (GSA) and channel guided attention (GCA) modules.

The attention modules compute alignment at the spatial and channel levels for the transformed pre-trained network feature map  $F_{P-tr}$  and the target network feature map  $F_T$ . The target network contains finite domain-specific knowledge through the labeled target subset, that can be leveraged to guide transfer learning. Hence, we empower the target network to choose or guide features from the teacher network that it deems suitable for transferring back to itself. We build a guided attention module to do this, which builds on the math synonymous to self-attention [64]. We wish to reflect that the notion of guided attention described in this paper is different from the concept of guided attention in [25,35,37], and is built on the idea described in co-attention [63]. Attention literature [55,60,11] describes the attention function as mapping a query and a set of key-value pairs to an output, where key, query, value, and output are all vectors. Since target features  $F_T$  guide the attention process, we designate transformed pre-trained network feature maps as the query vectors. Similarly, key and value are assigned to target network feature maps  $F_{P-tr}$ . Attention weights are computed as:

$$A = S(C_q(F_{P-tr}^\top) \odot C_k(F_T))^\top \odot C_v(F_T), \quad (1)$$

where  $\top$ ,  $S$ , and  $\odot$  denote transpose operation, softmax and matrix multiplication, respectively.  $C_k, C_q, C_v$  denote  $1 \times 1$  convolutions followed by reshaping of the key, query, and value feature maps respectively.

We incorporate the notion of guided spatial and channel attentions [60] using spatial and channel level feature vectors [11]. The goal of the Guided Spatial

Attention (GSA) module (which generates attention representations  $A_{GSA}$ ) is to highlight spatial regions of the transformed pre-trained network feature map,  $F_{P-tr}$  that align well with the target feature map,  $F_T$ . The goal of the Guided Channel Attention module (which generates attention representations  $A_{GCA}$ ) is to highlight attributes (or channel level features at each spatial location) of transformed source network features  $F_{P-tr}$  at each spatial location that align well with the target network feature maps  $F_T$ .

**Training GATN and Target Network:** We jointly train GATN, and the target network with the following loss terms:

- Transfer learning loss  $L_{Tr}$ :  $L_{Tr}$  is computed as the attention weighted mean squared difference between transformed pre-trained feature maps  $F_{P-tr}$  and target network feature maps  $F_T$ . The intuition is  $F_{P-tr}$  is aligned with  $F_T$ , and the extent to which these feature maps are aligned is delineated by the attention representations. This loss is applied to all target images (labeled as well as unlabeled) and scaled by a hyper-parameter  $\lambda_{Tr}$ , empirically chosen to 0.1 or 0.01 depending on the task. Specifically, we denote  $\lambda_{Tr,UL}$  and  $\lambda_{Tr,L}$  as the hyper-parameter on unlabeled and labeled target subsets respectively. Mathematically,

$$L_{Tr} = \sum A_{GSA} * [F_{P-tr} - F_T]^2 + \sum A_{GCA} * [F_{P-tr} - F_T]^2. \quad (2)$$

- Task specific loss  $L_{Task}$ : We apply traditional task losses on the output of target task head,  $TH_T$ , viz. multi-class cross entropy for classification and semantic segmentation, and focal loss for object detection, for the labeled subset of target domain images, and is scaled by a hyper-parameter  $\lambda_{pseudo}$  typically set to 1.0 [21].

### 2.3 The Active Learning Strategy $H_{AL}$

The effectiveness of GATN, and robustness and generalizability of the target network depends on the samples mined by the AL strategy  $H_{AL}$ , which strikes a fine balance between transferability from the pre-trained network, and pertinence w.r.t. to the target domain.

- *Transferability from the pre-trained network:* For compute the transferability score, we threshold the final softmax output of the pre-trained network,  $N_S$  is to compute pseudo label map for the target samples. The task-specific loss is computed between the softmax output and 1-hot encoding of the pseudo-label map for the source network. The transferability score,  $A_G$  is then taken to be the total  $l_2$  norm of the gradient (without any gradient update - since the network is frozen) over the pretrained network wrt the computed loss. Low gradient implies high confidence and hence high transferability from the source network.
- *Uncertainty of the target network:* The softmax output of the target network provides the class-wise probability score map  $\mathbf{p}$ . This is used to compute the entropy score  $AE$  as  $-\sum p \log p$ . High entropy for a target sample indicates high uncertainty and hence should be selected for labeling.

A combination of the above two measures is maximized greedily to mine the samples for labeling:

$$H_{AL} = -\lambda_G \log A_G + \lambda_E \log A_E \quad (3)$$

where  $\lambda_G, \lambda_E$ , are binary variables (0/1) that toggle the metrics used for sampling. For the first batch of AL, we set  $\lambda_G = 1$ , and  $\lambda_E = 0$ . This is because at the start of training, there is no knowledge available about the target dataset. Thus, we empirically decide to sample images that have good confidence with respect to the pre-trained network for the first round. For the subsequent rounds of sampling, we follow a simple weighting scheme where transferability and uncertainty are given equal importance.

Table 1: **Tasks and Datasets:** The source and target datasets are listed in the first two columns. The fourth column indicates whether there is a shift in label space while adapting from the source to the target domain.

Source	Target	Task	Label Shift	Eval.
MNIST [8]	SVHN [49]	Classification	No	Accuracy
SVHN [49]	MNIST [8]	Classification	No	Acc.
MNIST [8]	SVHN [49]	Classification	Yes (2 cases)	Acc.
GTA5 [42]	CityScapes [6]	Segmentation	No	Acc., IoU
Publaynet [66]	DSSE [62]	Document Layout Detection	Yes	mAP

### 3 Experiments and Results

We succinctly present the tasks, datasets, and evaluation metrics in Table 1. Under classification settings, DistillAdapt, even without access to annotated source data, performs similar to or better than (with a variance of 0.5% in accuracy) prior active domain adaptation methods [52,39] that use large amounts (more than 100k samples) of annotated source data. Furthermore, we conduct experiments on MNIST under 2 distinct cases of shift in output label space, and show that DistillAdapt can achieve atleast 99.4% of the accuracy obtained when there is no shift in label space. Thus, DistillAdapt can handle shifts in label space. Our experiments on CityScapes for semantic segmentation at various budgets reveal an improvement of atleast 5.57% over source-free fine-tuning (*i.e.* training the model without  $L_{tr}$ ). Finally, we conduct experiments on document layout adaptation from PubLayNet to DSSE where there is a shift in output label space, DistillAdapt imparts a relative improvement of 31.3% over fine-tuning (*i.e.* training the model without  $L_{tr}$ ). **Reproducibility:** We provide a detailed description of the datasets, hyperparameters and training details in the supplementary material. We also include the codes for GATN and  $H_{AL}$ , and links to external repositories to setup the datasets, task-specific training scripts along with detailed training instructions.

#### 3.1 Digits Classification

We present our results on digits classification datasets under two settings: (i) shared label space, and (ii) shift in label space. In the shared label space setting, the

Table 2: Results on digits classification in the shared label space setting

Method	Source Data	B=100	B=200	B=300
Source only accuracy: 62.25				
O-ALDA [45]	✓	79.10	81.40	82.70
CDAN [32] + Entropy [52]	✓	93.10	94.60	95.00
CDAN [32] + BvSB [52]	✓	94.20	95.00	95.90
CDAN [32] + Uniform [39]	✓	90.00	94.00	94.50
CDAN [32] + BADGE [2]	✓	92.90	94.90	96.50
SSDA MME [46]	✓	93.00	95.00	95.50
AADA [52]	✓	94.20	95.20	95.50
CLUE [39]	✓	95.50	96.20	96.50
DistillAdapt	✗	91.64	95.96	<b>97.16</b>

Method	1000	2000	4000	10000
Source only accuracy: 27.27				
FT+Uniform	68.0	76.2	80.0	84.7
FT+Entropy	68.0	75.1	81.2	87.8
FT+BADGE [2]	70.1	79.2	83.7	88.1
FT+Coreset [48]	70.0	78.8	82.8	88.2
FT+Margin [43]	71.0	78.0	83.2	88.4
FT+CLUE [39]	72.1	76.4	83.0	87.8
DistillAdapt	<b>74.2</b>	<b>82.2</b>	<b>86.6</b>	<b>88.6</b>

(a) **Results on adapting from SVHN to MNIST:** With a budget of 300 images (0.5% of target data MNIST, last column of table), we show that, even without source data, DistillAdapt outperforms prior work on active domain adaptation, using annotated source data.

(b) **Results on adapting from MNIST to SVHN:** We compare with prior methods on active learning, and demonstrate state-of-the-art performance.

label space that the pre-trained network was trained on and the label space of the target domains are the same. In the label space shift space setting, the target dataset contains labels not used for training the source network. We used Resnet-101 features for the experiment, consistent with the baselines. We set  $\lambda_{Tr} = 0.01$ , and  $\lambda_G$  to 1.0 and  $\lambda_E$  to 1.0 after first round of sampling. In addition, we generate pseudo-labels from the target network for the unlabeled subset and add it to the  $L_{task}$ . We use feature heads from the penultimate layer of the ResNet-101 classifier backbone.

Table 3: Comparing DistillAdapt with prior art on SFDA on digits datasets. Budget reflects the percentage of total number of target samples used for active learning. We demonstrate that our SF-ADA approach outperforms prior art on SFDA by a large margin using a very small proportion of annotated target samples.

Method	Budget	Accuracy
SDDA (WACV 2021) [23]	-	75.5
SDDA-P (WACV 2021) [23]	-	76.3
DistillAdapt	0.16%	91.64

Method	Budget	Accuracy
SDDA (WACV 2021) [23]	-	42.2
SDDA-P (WACV 2021) [23]	-	43.6
DistillAdapt	0.18%	74.2

(a) SVHN to MNIST

(b) MNIST to SVHN

**Shared label-space setting, SVHN to MNIST:** Table 2a contains results of adapting from SVHN to MNIST, at various budgets. Concurrent with our intuition, the accuracy is better at higher budgets. When benchmarked at a budget of 300 samples, which is 0.5% of the total samples that MNIST contains, we observe that DistillAdapt, even without any annotated source data, outperforms prior work on active domain adaptation which use large amounts of annotated source data (600000 images). Moreover, we observe that the accuracy of 97.16% with 300 images is 97.64% of fully supervised accuracy with 60000 images. Our SF-ADA method outperforms prior work on ADA. Since ADA (or AL + DA) methods are better than AL + SFDA methods, by transitivity, a holistic solution for SF-ADA is more beneficial than a naive combination of SFDA and AL.

**Shared label-space setting, MNIST to SVHN:** We show results on adaptation from MNIST to SVHN in Table 2b. The complexity of SVHN is higher than that of MNIST, reflected in the source-only accuracy which stands at 27%. As per the prior work, we cap the net budget for mining samples via active learning at 10000 images, which is 1.8% of the total size of the dataset. We demonstrate state-of-the-art performance at varying budget of 1000, 2000, 4000 and 10000 images. Moreover, the accuracy at 10000 images is 93.44% of fully supervised accuracy, which uses almost 555,555 images.

Table 4: **Results on adaptation from SVHN to MNIST, for label space shift.** We consider two scenarios: case 1 - source data does not contain digits ‘3’ and ‘9’, case 2 - source data does not contain digits ‘7’, ‘5’, ‘4’, ‘1’. DistillAdapt, with  $H_{AL}$  and GATN, achieves 99.4% and 99.8% of the accuracy in the scenario with no label shift. The accuracy at a budget of 300 images, without label shift, is 97.16%

Class/Exp.	mean	0	1	2	3	4	5	6	7	8	9
Case 1: Remove the digits ‘3’ and ‘9’ from source SVHN											
Source only	56.88	69.20	86.80	79.10	0.00	53.80	95.70	41.00	78.20	63.00	0.00
B=100	88.29	97.80	98.90	94.60	83.80	94.30	96.60	84.90	91.00	93.80	48.20
B=200	96.27	98.50	98.60	98.10	94.30	96.70	97.80	97.90	93.60	92.80	94.40
B=300	96.61	99.10	98.70	98.10	95.00	97.50	97.90	98.00	91.30	95.40	97.10
Case 2: Remove the digits ‘7’, ‘5’, ‘4’, ‘1’ from source SVHN											
Source only	41.90	0.00	70.80	65.60	89.60	0.00	0.00	83.00	0.00	66.00	47.60
B=100	87.11	98.80	99.40	93.80	97.30	82.70	49.90	94.20	85.60	66.40	95.40
B=200	92.53	97.60	98.90	94.10	97.40	96.10	60.80	95.90	90.50	94.50	94.60
B=300	97.00	99.20	98.90	97.20	99.10	96.20	95.70	97.50	95.30	94.70	96.30

**Shift in label space, SVHN to MNIST:** In Table 4, we present results on adapting from SVHN to MNIST under a shift in label space. In case 1, we train the source network on SVHN after removing samples corresponding to two classes (class 3 and class 9, randomly chosen). Similarly, in case 2, we remove 4 classes from the source dataset. Direct testing reveals that the accuracy for these classes is 0. Sampling with our AL strategy §2.2 and gradually training with GATN gradually up to a budget of 300 images (again, 0.5% of target samples) restores accuracy to 96.61% and 97.00%, respectively, which is 99.4% and 99.8% of the accuracy achieved in the scenario with no label shift. Thus, our method works well when there is a shift in label space.

Table 5: Ablation Experiments on adaptation from SVHN to MNIST

GATN Specification		AL Specification		Budget	Acc
$\lambda_{Tr,UL}$	$\lambda_{Tr,UL}$	$A_G$	$A_E$		
Baseline source-free accuracy: 62.25%					
0	0	✓	✗	300	88.96
0	0.01	✓	✗	300	89.56
0.01	0.01	✓	✗	300	92.56
0.01	0.01	✓	✓	300	97.16

**Ablation experiments:** We present ablation experiments on adaptation from SVHN to MNIST in Table 5. We set the net active learning budget at 300 images.

Since the network has no prior knowledge about the target domain, the uncertainty metric can be applied only from the second round of active sampling. In the first round of active sampling, we apply only the transferability metric. In the first experiment, we study the impact of training the target network, without GATN, with all samples mined using just the transferability score, the accuracy is 88.96. This proves that even in the absence of knowledge transfer from the pre-trained network, samples mined using the pretrained networks’ confidence score is advantageous since the target network is initialized with the weights of the pretrained network. Next, we apply the distillation loss dictated by GATN only on the labeled subset and correspondingly set  $L_{L,Tr} = 0.01$ . We observe that knowledge transfer, in addition to sampling using the transferability score improves performance by 0.6%, on an absolute scale. This reinforces the quality of samples mined by the pretrained network. Next, we apply the distillation loss to the unlabeled subset as well ( $L_{Tr,UL}$ ), which leads to an absolute improvement of 3%. This is an indicator of GATN’s selective knowledge distillation capabilities, where only useful features are distilled to cumulatively improve performance. Finally, we experiment by using the uncertainty score, as well as the diversity score, to achieve an accuracy of 97.16%, an absolute improvement of 34.91% over the baseline and an absolute improvement of 5.6% over Experiment 3. Hence, the best knowledge transfer using GATN is obtained when samples are mined intelligently (Experiment 4).

Table 6: **GTA5 to CityScapes Adaptation:** We show that DistillAdapt imparts a relative improvement of 31.5%, 46.03%, 52.5% and 62.1% over the baseline source model with budgets of 50, 100, 200, and 500 images, with  $3 \times -25 \times$  improvement on specific classes like “Bike”, “Train”, “MBike”, “Sidewalk”, etc.

Experiment	mIoU	mAcc	Road	Sidewalk	Building	Wall	Fence	Pole	Light	Sign	Veg	Terrain	Sky	Person	Rider	Car	Truck	Bus	Train	MBike	Bike
Source only	34.91	77.84	70.14	21.6	76.27	18.8	16.27	21.31	27.85	15.40	77.67	31.29	74.83	49.47	3.60	79.45	28.71	31.39	4.70	12.43	2.10
TENT [58] (Source-free)	38.9	-	87.3	39.0	79.8	24.3	19.6	21.2	25.1	16.6	83.8	34.7	77.7	57.9	17.8	85.0	24.9	20.8	2.0	16.6	4.5
S4T [40] (Source-free)	43.98	-	88.2	44.2	84.4	28.9	27.6	38.6	41.5	8.4	86.3	41.0	79.2	58.7	25.3	85.4	20.1	26.4	6.3	10.8	8.4
B=50	45.93	89.22	92.09	52.57	83.43	23.72	18.37	33.33	35.90	44.01	84.24	39.23	85.82	55.39	20.16	84.02	38.57	37.77	2.72	16.09	25.26
B=100	50.98	90.33	93.6	57.79	84.16	23.4	21.98	36.07	38.12	45.8	85.39	41.33	86.34	57.67	30.41	86.1	43.81	45.02	26.02	19.15	46.48
B=200	53.34	91.18	94.82	63.83	85.29	29.01	27.85	36.84	39.84	47.53	86.33	42.16	88.4	60.16	31.85	86.88	48.64	48.45	26.29	20.46	48.91
B=500	56.59	92.09	95.59	68.77	86.41	33.08	34.88	39.49	42.54	52.44	87.30	48.17	89.73	62.96	33.91	88.18	53.67	52.41	29.08	23.46	53.15

### 3.2 Synthetic to Real Segmentation on CityScapes

We conduct experiments on a dense pixel-level task, segmentation, where we adapt from GTA5 (25000 images) to CityScapes. To effectively transfer from GTA5 and address uncertainty of the target network while sampling, we set  $\lambda_G = \lambda_E = 1$  from the second round of sampling. We set  $\lambda_{Tr} = 0.01$ . We use feature heads from the layer 3 of the underlying DeepLabv2 ResNet-101 backbone [5]. We present the results in Table 6. In the first row, we directly test the pre-trained GTA5 model, which gives an mIoU of 34.91. We next apply  $H_{AL}$  for batch active learning, and train the network using GATN after each round of sampling. A cumulative budget of 50 images, 100 images, 200 images, and 500 images leads to relative improvements (over the source only mIoU) of 31.5%, 46.03%, 52.5% and 62.1% respectively. Classes like ‘Sidewalk’, ‘Wall’, ‘Fence’,

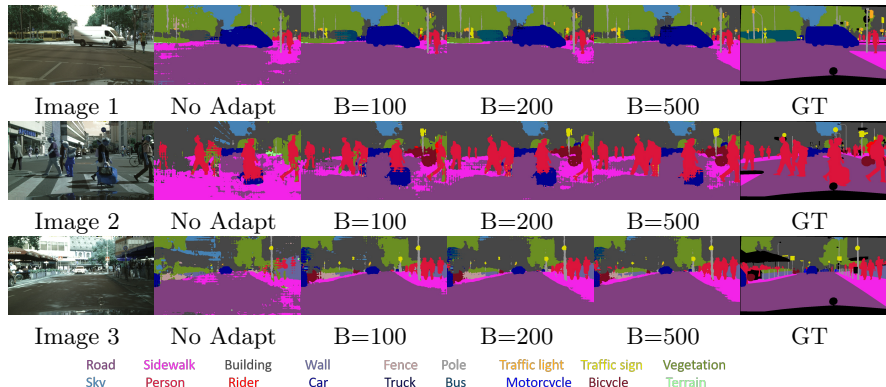


Fig. 2: **Qualitative results on the CityScapes dataset.** The second column has results before adaptation. The next three columns show results on adaptation with budgets of 100, 200, and 500 images respectively. The last column shows the groundtruth. Classes like sidewalk, train, pedestrians, buildings, road, and cars are detected better after adaptation with DistillAdapt .

‘Pole’, ‘Sign’, ‘Rider’, ‘Train’, ‘MBike’, ‘Bike’ have very low mIoU ( $\sim 20\%$  or less) when directly transferred from the source model. We show that DistillAdapt improves performance by  $3 \times -25\times$ . Classwise comparisons with prior art on SFDA reveal that our AL heuristic  $H_{AL}$  strategically chooses classes like Bike and MBike with low confidence or high uncertainty to boost performance, while not compromising on performance w.r.t. transferable classes like road and sky.

Table 7: **Comparisons with the state-of-the-art SFDA approaches for adaptation from GTA to CityScapes.** We show that DistillAdapt achieves state-of-the-art mIoU with a small budget of 50 images, the mIoU obtained by naive finetuning [59] on 50 images is 39.5.

Method	mIoU
UBNA [19] (WACVW 2022)	36.1
UBNA+ [19] (WACVW 2022)	36.5
TENT [58] (ICLR 2021)	38.86
TENT + MS [58] (ICLR 2021)	36.89
SFDA (w/o IPSP) [30] (CVPR 2021)	41.35
SFDA [30] (CVPR 2021)	43.16
URMA [9] (CVPR 2021)	45.1
S4T [40] (ArXiv 2021)	43.98
S4T + MS [40] (ArXiv 2021)	44.83
<b>DistillAdapt</b>	<b>45.93</b>

**Comparisons with SFDA methods:** Table 7 shows the comparison of DistillAdapt with prior SFDA methods. DistillAdapt performs better with a budget of only 50 images (1.5%).

**Ablation experiments:** We present ablation experiments in Table 8. In Table 8(a), we study the effectiveness of GATN at various budgets. In the second column, we apply the transfer learning loss dictated by GATN to only the labeled subset, along with active learning using  $H_{AL}$ . The third column reflects mIoUs obtained by using our complete model, applying the transfer learning on labeled

Table 8: **Ablation experiments for adaptation from GTA5 to CityScapes.** In table (a), we study ablations on transfer loss for GATN, Table (b) shows ablations on GATN components at a budget of 50 images. In table (c), we ablate on the active learning heuristic,  $H_{AL}$  at a budget of 500 images.

Budget $B$ ( $\lambda_{Tr,L}$ , $\lambda_{Tr,UL}$ ) (0.1,0) (0.1,0.1)			GSA GCA mIoU			$H_{AL}$ mIoU	
50	44.62	45.93	✗	✗	39.50	$A_G$	50.29
100	48.72	50.98	✓	✗	45.43	$A_G + A_E$	56.59
200	50.49	53.34	✗	✓	45.45		
500	53.46	56.59	✓	✓	45.93		

(a) (b) (c)

Table 9: **Adaptation for document layout detection from PubLayNet to DSSE:** Fine-tuning with DistillAdapt improves performance by 31.3% over fine-tuning without DistillAdapt.

Experiment	mAP	Text	Caption	Figure	Table	List	Section
FT w/o DistillAdapt	23.11	36.12	13.49	25.60	22.24	29.57	11.64
FT w. DistillAdapt	30.36	44.59	11.61	35.57	24.80	37.48	28.18

as well as unlabeled subsets along with active learning using  $H_{AL}$ . A comparison of the second and third columns indicates the benefits of selective transfer learning using GATN. Moreover, our model results in relative improvements of 16.27%, 16.92%, 13.24% and 5.57% over the baseline numbers [59] obtained by naively finetuning the target network (with pre-trained weights initialization) without GATN, and by random sampling [59], at budgets of 50 images, 100 images, 200 images, and 500 images respectively. In Table 8(b), we study the effectiveness of the different components of GATN, at a budget of 50 images. In the first experiment, we do not use either GCA or GSA [59]. Without GATN, our system will reduce to simple fine-tuning of the target network with the annotated target samples. GATN forms a bridge between the pre-trained network and the target network, and removing it would break the knowledge transfer process. In the subsequent experiments, we show the impact of using channel and spatial features. In Table 8(c), we demonstrate the effectiveness of using the fusion AL heuristic comprising of the transferability score w.r.t. the pretrained network as well as the uncertainty score w.r.t. the target network, as opposed to using just the transferability score.

### 3.3 Document Layout Detection: DSSE

In this section, we adapt from the medical documents dataset PubLayNet to documents belonging to DSSE, a dataset containing magazines, receipts and posters. The documents in the two domains are quite different. Medical documents are written in a two-column format, with uniform text, figures and tables. In contrast, the target domain, DSSE, a new unseen dataset, is small (only 150 documents) and is extremely diverse. Moreover, PubLayNet has 5 classes, while

DSSE has 6 classes. Hence, there is a *shift* in label space. Direct testing of PubLayNet on DSSE results in a mAP of 15.67. Since the dataset is very small, we do not apply  $H_{AL}$ , and instead directly use all 150 images for GATN. We use feature heads from the FPN of the underlying RetinaNet ResNet-101 backbone [29]. Fine-tuning without DistillAdapt results in a mAP of 23.11, and fine-tuning with DistillAdapt improves performance by 31.3% to 30.36.

Table 10: **Problem Settings:** We highlight various domain adaptation settings. Src. Data, Src. Model, Lab. Tar., and Un. Tar. refer to abundant labeled source data, Source Model, Scarce Labeled Target Data and Unlabeled Abundant Target Data, respectively.

Problem	Src. Data	Src. Model	Lab. Tar.	Un. Tar.
Semi Supervised DA (SSDA) [59]	✓	✓	✓	✓
Unsupervised DA (UDA) [53]	✓	✓	✗	✓
Source-Free DA (SFDA) [22]	✗	✓	✗	✓
Active DA (ADA) [52]	✓	✓	✓	✓
Source Free Active DA (SF-ADA)	✗	✓	✓	✓

## 4 Related Work

There is significant prior work on active learning, domain adaptation, and active domain adaptation. However, to the best of our knowledge, there is not much prior work on active domain adaptation without source data.

**Active Learning** Active Learning (AL) aims to acquire a given small budget of labeled data while maximizing supervised training performance. Uncertainty-based methods select examples with the highest uncertainty under the current model [57,43], using entropy [57], minimum classification margins [43], least confidence, etc. Diversity-based methods choose some points representative of the data, e.g. core-set selection [48,51]. Recent approaches combine these two paradigms [2,39,65].

**Domain Adaptation** Domain adaptation aims to transfer the knowledge learned by a source domain model to an unlabeled target domain. Some of the existing works align feature spaces of the source and target domains by learning domain invariant feature representations by divergence-based measure minimization [17,31], adversarial training [47,50,54], source or target domain data reconstruction [3,12], image-to-image translation [33,13] or normalization statistics [34,27]. However, domain adaptation methods typically require access to annotated source data.

**Source-free Domain Adaptation** [26] introduced the paradigm of domain adaptation where source domain data is not available due to privacy issues and only a model pre-trained on the source domain data is available. Existing works employ a generative approach where the trained model is used to generate source samples using batch normalization [15] or energy-based methods [23] for classification task [61,18,1]. Others use a combination of distillation-based approach [30] or information maximization-based approach [28]. However, these methods do not consider using active learning to boost the performance, and typically do not generalize across tasks.

**Active Domain Adaptation** Active domain adaptation aims to adapt a model trained on source domain data to target domain by annotating a fixed budget of target domain samples. [41] introduced the task of ADA with applications to sentiment classification for textual data. They proposed a method employing a sampling strategy based on model uncertainty and a learned domain separator. More recently, [52] studied ADA in the context of CNN’s and proposed a method wherein samples are selected based on their uncertainty and target-ness, followed by adversarial domain adaptation. [46] proposed an algorithm that identifies uncertain and diverse instances for labeling followed by semi-supervised DA. [67] proposed a three-stage active adversarial training of neural networks using invariant feature space learning, uncertainty and diversity-based criteria for sample selection and re-training. [4] addressed the problem of lack of guarantee of good transfer-ability of features in domain adaptation. However, all of the above works use source domain data.

#### 4.1 Comparisons with Related Work

In Table 10, we present various domain adaptation problem settings. In this paper, we propose an architecture for source-free active domain adaptation (SF-ADA). On one hand, SF-ADA can be seen as ADA [39,10] without source data. It can also be seen as an amalgamation of the notions of SFDA [26,28] and AL [4]. SF-ADA requires DistillAdapt to address knowledge transfer from the pre-trained network and acquiring samples for annotation in a complementary manner. The design of GATN incorporates the transfer mechanism with spatial and channel attention [60,11]. We wish to reflect that our novelty is in the formulation of guided attention, rather than spatial and channel attention. Similarly, we wish to highlight that the AL heuristic  $H_{AL}$  builds on the notion of entropy and gradient computation and is customized to the problem of SF-ADA.

### 5 Conclusions, Limitations and Future Work

We propose a novel method, DistillAdapt, for Source-Free Active Domain Adaptation. DistillAdapt consists of two key components: an active learning strategy  $H_{AL}$ , and GATN for effective transfer learning and sampling. We evaluate the performance across 3 tasks and highlight the benefits of DistillAdapt. Overall, DistillAdapt is a task-agnostic and label-agnostic approach that does not require source data. Moreover, both the pre-trained and GATN networks are not needed during the evaluation stage. We expect that DistillAdapt for SF-ADA can be extended to varied tasks like cross-lingual question answering, domain stylization, etc. Using learnable weights for the scores in the active learning heuristic could also be an interesting direction for future work.

### 6 Datasets

In this section, we describe the datasets used in our experiments.

### 6.1 Classification

- MNIST [8]: MNIST is a handwritten digits dataset, with 60,000 samples for training and 10,000 samples for testing. It can be downloaded at <http://yann.lecun.com/exdb/mnist/>.
- SVHN [49]: SVHN is a house street numbers dataset, and has cropped digits with character wise ground-truth in MNIST format. It has over 600,000 images and is a much more realistic dataset than MNIST. It can be downloaded at <http://ufdl.stanford.edu/housenumbers/>.
- VISDA-17 [38]: VISDA is dataset designed for synthetic to real adaptation. The synthetic images are 2D renderings of 3D models generated from various angles and lighting conditions. The real images correspond to natural scene objects. It can be downloaded at <http://ai.bu.edu/visda-2017/>.

### 6.2 Segmentation

- GTA5 [42]: GTA5 is a synthetic driving dataset extracted from the computer game Grand Theft Auto. It has 25000 high resolution images. The dataset is available at [https://download.visinf.tu-darmstadt.de/data/from\\_games/](https://download.visinf.tu-darmstadt.de/data/from_games/). It has 19 classes compatible with CityScapes.
- CityScapes [6]: CityScapes is a real driving dataset collected in Europe. It has 2975 high resolution images for training, and 500 images for testing. The dataset is available for download at <https://www.cityscapes-dataset.com/>. It has 19 classes.

### 6.3 Document Layout Detection

- PubLayNet [66]: PubLayNet is a large-scale medical documents dataset consisting of images of pages extracted from scientific medical papers. Medical documents are written in a two-column format, with uniform text, figures and tables. It has 360,000 images and 5 classes. The dataset can be downloaded at <https://github.com/ibm-aur-nlp/PubLayNet>.
- DSSE [62]: DSSE contains images of pages extracted from magazines, receipts and posters. DSSE is a small dataset with just 150 documents, and has 6 classes, paving way for open-set adaptation from DSSE. The dataset can be downloaded at [http://personal.psu.edu/xuy111/projects/cvpr2017\\_doc.html](http://personal.psu.edu/xuy111/projects/cvpr2017_doc.html).

## 7 Synthetic to Real VISDA17 Classification


We conduct experiments on the popular VISDA17 dataset for synthetic to real adaptation. For effective transfer, and to address uncertainty of the target network while sampling, we set  $\lambda_G = \lambda_E = 1$  from the second round of sampling. VISDA is a huge dataset with a large variety of samples. Hence, we factor in diversity. The output feature  $F_T$  for target samples for clustered using k-means [2]. The mean distance of each target sample from the previously annotated target points gives the diversity score  $A_D$ . We set the hyperparameter for diversity

Table 11: **Synthetic to Real Classification on VISDA:** Our source-free method is on par with state-of-the-art methods that use abundant annotated source data (more than 100k samples).

Method	Source Data	B=10%	B=20%
Random	✓	82.1	87.2
UCN [16]	✓	85.4	90.3
QBC [36]	✓	84.1	89.6
Cluster [7]	✓	83.5	89.6
AADA [52]	✓	84.6	89.7
ADMA [14]	✓	84.8	90.0
DistillAdapt	✗	84.8	89.3

score  $\lambda_K = 1$  from the second round of sampling. On budgets of 10%, and 20% of the total target samples, we achieve accuracies of 84.8% and 89.3% respectively. Though DistillAdapt does not use any annotated source data, it achieves accuracies on par with prior work using abundant annotated source data (more than 100k samples).

Table 12: **MNIST Results:** The handwritten digit examples shown here were misclassified initially by the pretrained source network. After the first round of DistillAdapt with a budget of 100 labeled samples, three out of six examples get correctly classified. In the next round, two more examples get correctly predicted and in the final round with a cumulative budget of 300 samples, all the examples shown here get classified correctly.

Image	0	100	200	300
	1	3	3	5
	0	3	3	3
	2	7	7	7
	1	3	2	2
	1	4	4	4
	1	3	2	2

## 8 Implementation details

*Hyperparameters:* The transformation network  $\tau$  is a four layer convolutional neural network with kernel size 3, and dilation and padding set to 1. The weight hyperparameter for  $L_{Tr}$  is set to 0.1. Our classification models are trained using 1 GPU with 16GB memory. Our document layout detection and segmentation models are trained using 8 GPUs with 16 GB memory each. All our codes are written using the PyTorch framework. For CityScapes, all images are downsampled by a factor of 2 using bilinear downsampling. Ground truth maps are downsampled by nearest neighbour downsampling. We retain the input image size for our classification experiments. For document layout detection, we resize

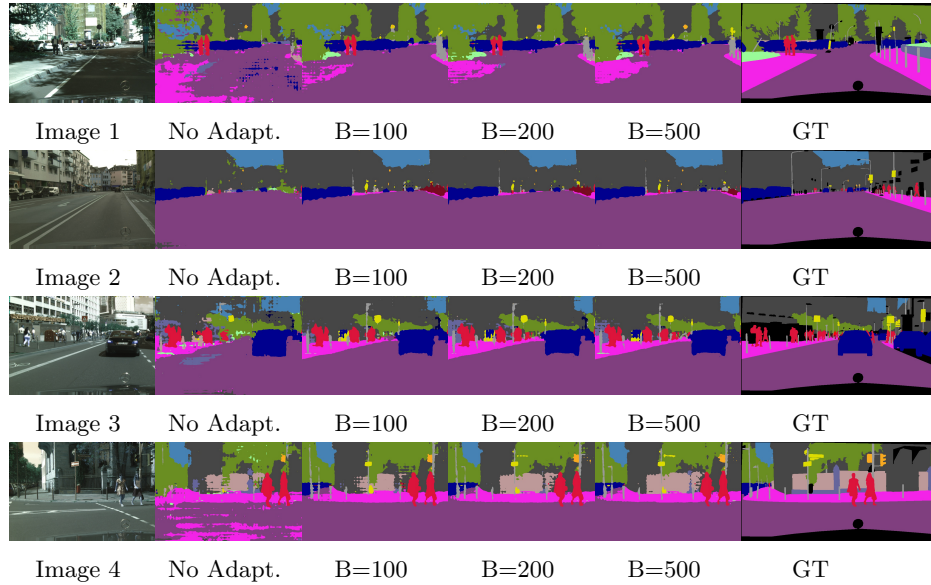


Fig. 3: **Qualitative results on the CityScapes dataset.** The second column has results before adaptation. The next three columns show results on adaptation with budgets of 100, 200, and 500 images respectively. The last column shows the ground truth. Classes like sidewalk, train, pedestrians, buildings, road, and cars are detected better after adaptation with DistillAdapt .

the images (and appropriately scale the bounding box coordinates) such that the length of the largest size does not exceed 500.

*Codes:* In the interest of reproducibility, we release the codes for GATN, including the code for the transformation network, the guided attention modules, and their incorporation within DeepLabv2 for segmentation. We release the train and eval scripts for segmentation as well. We also provide the scripts for  $H_{AL}$  with the supplementary zip file. We will make these scripts publicly available upon acceptance of the paper.

We also provide the links to public repositories that we used in our experiments for running DistillAdapt experiments.

– Classification

- Backbone network: <https://github.com/tim-learn/SHOT/blob/master/object/network.py>  
Please follow the procedure in the `deeplab_multi.py` script in the supplementary zip file to incorporate GATN within the classification backbone.
- MNIST and SVHN dataloader: [https://github.com/tim-learn/SHOT/tree/master/digit/data\\_load](https://github.com/tim-learn/SHOT/tree/master/digit/data_load)
- VISDA dataloader: <https://github.com/VisionLearningGroup/taskcv-2017-public>
- Training and eval scripts: Please modify the train and eval script in the supplementary zip file to modify code for classification.

- Document Layout Detection
  - Backbone network, train and test scripts: <https://github.com/yhenon/pytorch-retinanet>
  - PubLayNet dataloader: [https://github.com/phamquiluan/PubLayNet/blob/master/training\\_code/datasets/publaynet.py](https://github.com/phamquiluan/PubLayNet/blob/master/training_code/datasets/publaynet.py)
  - DSSE dataloader: Use the PubLayNet dataloader to modify.
- Semantic Segmentation
  - Backbone network, train and test scripts: Please check the supplementary zip file.
  - GTA5 and CityScapes dataloaders: <https://github.com/wasidennis/AdaptSegNet/tree/master/dataset>

## References

1. Agarwal, P., Paudel, D.P., Zaech, J.N., Van Gool, L.: Unsupervised robust domain adaptation without source data. In: *Proceedings of the IEEE/CVF Winter Conference on Applications of Computer Vision*. pp. 2009–2018 (2022)
2. Ash, J.T., Zhang, C., Krishnamurthy, A., Langford, J., Agarwal, A.: Deep batch active learning by diverse, uncertain gradient lower bounds. *arXiv preprint arXiv:1906.03671* (2019)
3. Bousmalis, K., Trigeorgis, G., Silberman, N., Krishnan, D., Erhan, D.: Domain separation networks. *Advances in neural information processing systems* **29**, 343–351 (2016)
4. Bouvier, V., Very, P., Chastagnol, C., Tami, M., Hudelot, C.: Stochastic adversarial gradient embedding for active domain adaptation. *arXiv preprint arXiv:2012.01843* (2020)
5. Chen, L.C., Papandreou, G., Schroff, F., Adam, H.: Rethinking atrous convolution for semantic image segmentation. *arXiv preprint arXiv:1706.05587* (2017)
6. Cordts, M., Omran, M., Ramos, S., Rehfeld, T., Enzweiler, M., Benenson, R., Franke, U., Roth, S., Schiele, B.: The cityscapes dataset for semantic urban scene understanding. In: *Proceedings of the IEEE conference on computer vision and pattern recognition*. pp. 3213–3223 (2016)
7. Dagan, I., Engelson, S.P.: Committee-based sampling for training probabilistic classifiers. In: *Machine Learning Proceedings 1995*, pp. 150–157. Elsevier (1995)
8. Deng, L.: The mnist database of handwritten digit images for machine learning research [best of the web]. *IEEE Signal Processing Magazine* **29**(6), 141–142 (2012)
9. Fleuret, F., et al.: Uncertainty reduction for model adaptation in semantic segmentation. In: *Proceedings of the IEEE/CVF Conference on Computer Vision and Pattern Recognition*. pp. 9613–9623 (2021)
10. Fu, B., Cao, Z., Wang, J., Long, M.: Transferable query selection for active domain adaptation. In: *Proceedings of the IEEE/CVF Conference on Computer Vision and Pattern Recognition*. pp. 7272–7281 (2021)
11. Fu, J., Liu, J., Tian, H., Li, Y., Bao, Y., Fang, Z., Lu, H.: Dual attention network for scene segmentation. In: *Proceedings of the IEEE/CVF Conference on Computer Vision and Pattern Recognition*. pp. 3146–3154 (2019)
12. Ghifary, M., Kleijn, W.B., Zhang, M., Balduzzi, D., Li, W.: Deep reconstruction-classification networks for unsupervised domain adaptation. In: *European conference on computer vision*. pp. 597–613. Springer (2016)

13. Hong, W., Wang, Z., Yang, M., Yuan, J.: Conditional generative adversarial network for structured domain adaptation. In: Proceedings of the IEEE Conference on Computer Vision and Pattern Recognition. pp. 1335–1344 (2018)
14. Huang, S.J., Zhao, J.W., Liu, Z.Y.: Cost-effective training of deep cnns with active model adaptation. In: Proceedings of the 24th ACM SIGKDD International Conference on Knowledge Discovery & Data Mining. pp. 1580–1588 (2018)
15. Ishii, M., Sugiyama, M.: Source-free domain adaptation via distributional alignment by matching batch normalization statistics. arXiv preprint arXiv:2101.10842 (2021)
16. Joshi, A.J., Porikli, F., Papanikolopoulos, N.P.: Scalable active learning for multiclass image classification. *IEEE transactions on pattern analysis and machine intelligence* **34**(11), 2259–2273 (2012)
17. Kang, G., Jiang, L., Yang, Y., Hauptmann, A.G.: Contrastive adaptation network for unsupervised domain adaptation. In: Proceedings of the IEEE/CVF Conference on Computer Vision and Pattern Recognition. pp. 4893–4902 (2019)
18. Kim, Y., Cho, D., Han, K., Panda, P., Hong, S.: Domain adaptation without source data. arXiv preprint arXiv:2007.01524 (2020)
19. Klingner, M., Termöhlen, J.A., Ritterbach, J., Fingscheidt, T.: Unsupervised batchnorm adaptation (ubna): A domain adaptation method for semantic segmentation without using source domain representations. In: Proceedings of the IEEE/CVF Winter Conference on Applications of Computer Vision. pp. 210–220 (2022)
20. Kothandaraman, D., Chandra, R., Manocha, D.: Ss-sfda: Self-supervised source-free domain adaptation for road segmentation in hazardous environments. arXiv preprint arXiv:2012.08939 (2020)
21. Kothandaraman, D., Nambiar, A.M., Mittal, A.: Domain adaptive knowledge distillation for driving scene semantic segmentation. In: WACV (Workshops). pp. 134–143 (2021)
22. Kundu, J.N., Venkat, N., Babu, R.V., et al.: Universal source-free domain adaptation. In: Proceedings of the IEEE/CVF Conference on Computer Vision and Pattern Recognition. pp. 4544–4553 (2020)
23. Kurmi, V.K., Subramanian, V.K., Namboodiri, V.P.: Domain impression: A source data free domain adaptation method. In: Proceedings of the IEEE/CVF Winter Conference on Applications of Computer Vision. pp. 615–625 (2021)
24. Li, K., Wigington, C., Tensmeyer, C., Zhao, H., Barmpalios, N., Morariu, V.I., Manjunatha, V., Sun, T., Fu, Y.: Cross-domain document object detection: Benchmark suite and method. In: Proceedings of the IEEE/CVF Conference on Computer Vision and Pattern Recognition. pp. 12915–12924 (2020)
25. Li, K., Wu, Z., Peng, K.C., Ernst, J., Fu, Y.: Guided attention inference network. *IEEE transactions on pattern analysis and machine intelligence* **42**(12), 2996–3010 (2019)
26. Li, R., Jiao, Q., Cao, W., Wong, H.S., Wu, S.: Model adaptation: Unsupervised domain adaptation without source data. In: Proceedings of the IEEE/CVF Conference on Computer Vision and Pattern Recognition. pp. 9641–9650 (2020)
27. Li, Y., Wang, N., Shi, J., Hou, X., Liu, J.: Adaptive batch normalization for practical domain adaptation. *Pattern Recognition* **80**, 109–117 (2018)
28. Liang, J., Hu, D., Wang, Y., He, R., Feng, J.: Source data-absent unsupervised domain adaptation through hypothesis transfer and labeling transfer. *IEEE Transactions on Pattern Analysis and Machine Intelligence* (2021)

29. Lin, T.Y., Goyal, P., Girshick, R., He, K., Dollár, P.: Focal loss for dense object detection. In: Proceedings of the IEEE international conference on computer vision. pp. 2980–2988 (2017)
30. Liu, Y., Zhang, W., Wang, J.: Source-free domain adaptation for semantic segmentation. In: Proceedings of the IEEE/CVF Conference on Computer Vision and Pattern Recognition. pp. 1215–1224 (2021)
31. Long, M., Cao, Y., Wang, J., Jordan, M.: Learning transferable features with deep adaptation networks. In: International conference on machine learning. pp. 97–105. PMLR (2015)
32. Long, M., Cao, Z., Wang, J., Jordan, M.I.: Conditional adversarial domain adaptation. arXiv preprint arXiv:1705.10667 (2017)
33. Mao, X., Li, Q.: Unpaired multi-domain image generation via regularized conditional gans. arXiv preprint arXiv:1805.02456 (2018)
34. Maria Carlucci, F., Porzi, L., Caputo, B., Ricci, E., Rota Bulò, S.: Autodial: Automatic domain alignment layers. In: Proceedings of the IEEE International Conference on Computer Vision. pp. 5067–5075 (2017)
35. Mun, J., Cho, M., Han, B.: Text-guided attention model for image captioning. In: Proceedings of the AAAI Conference on Artificial Intelligence. vol. 31 (2017)
36. Nguyen, H.T., Smeulders, A.: Active learning using pre-clustering. In: Proceedings of the twenty-first international conference on Machine learning. p. 79 (2004)
37. Pang, Y., Xie, J., Khan, M.H., Anwer, R.M., Khan, F.S., Shao, L.: Mask-guided attention network for occluded pedestrian detection. In: Proceedings of the IEEE/CVF International Conference on Computer Vision. pp. 4967–4975 (2019)
38. Peng, X., Usman, B., Kaushik, N., Hoffman, J., Wang, D., Saenko, K.: Visda: The visual domain adaptation challenge. arXiv preprint arXiv:1710.06924 (2017)
39. Prabhu, V., Chandrasekaran, A., Saenko, K., Hoffman, J.: Active domain adaptation via clustering uncertainty-weighted embeddings. arXiv preprint arXiv:2010.08666 (2020)
40. Prabhu, V., Khare, S., Kartik, D., Hoffman, J.: S4t: Source-free domain adaptation for semantic segmentation via self-supervised selective self-training. arXiv preprint arXiv:2107.10140 (2021)
41. Rai, P., Saha, A., Daumé III, H., Venkatasubramanian, S.: Domain adaptation meets active learning. In: Proceedings of the NAACL HLT 2010 Workshop on Active Learning for Natural Language Processing. pp. 27–32 (2010)
42. Richter, S.R., Vineet, V., Roth, S., Koltun, V.: Playing for data: Ground truth from computer games. In: European conference on computer vision. pp. 102–118. Springer (2016)
43. Roth, D., Small, K.: Margin-based active learning for structured output spaces. In: European Conference on Machine Learning. pp. 413–424. Springer (2006)
44. Rusticus, D., Goldmann, L., Reisser, M., Villegas, M.: Document domain adaptation with generative adversarial networks. In: 2019 International Conference on Document Analysis and Recognition (ICDAR). pp. 1432–1437. IEEE (2019)
45. Saha, A., Rai, P., Daumé, H., Venkatasubramanian, S., DuVall, S.L.: Active supervised domain adaptation. In: Joint European Conference on Machine Learning and Knowledge Discovery in Databases. pp. 97–112. Springer (2011)
46. Saito, K., Kim, D., Sclaroff, S., Darrell, T., Saenko, K.: Semi-supervised domain adaptation via minimax entropy. In: Proceedings of the IEEE/CVF International Conference on Computer Vision. pp. 8050–8058 (2019)
47. Sankaranarayanan, S., Balaji, Y., Castillo, C.D., Chellappa, R.: Generate to adapt: Aligning domains using generative adversarial networks. In: Proceedings of the

- IEEE Conference on Computer Vision and Pattern Recognition. pp. 8503–8512 (2018)
48. Sener, O., Savarese, S.: Active learning for convolutional neural networks: A core-set approach. arXiv preprint arXiv:1708.00489 (2017)
  49. Sermanet, P., Chintala, S., LeCun, Y.: Convolutional neural networks applied to house numbers digit classification. In: Proceedings of the 21st International Conference on Pattern Recognition (ICPR2012). pp. 3288–3291. IEEE (2012)
  50. Shen, J., Qu, Y., Zhang, W., Yu, Y.: Wasserstein distance guided representation learning for domain adaptation. In: Thirty-Second AAAI Conference on Artificial Intelligence (2018)
  51. Sinha, S., Ebrahimi, S., Darrell, T.: Variational adversarial active learning. In: Proceedings of the IEEE/CVF International Conference on Computer Vision. pp. 5972–5981 (2019)
  52. Su, J.C., Tsai, Y.H., Sohn, K., Liu, B., Maji, S., Chandraker, M.: Active adversarial domain adaptation. In: Proceedings of the IEEE/CVF Winter Conference on Applications of Computer Vision. pp. 739–748 (2020)
  53. Tsai, Y.H., Hung, W.C., Schuster, S., Sohn, K., Yang, M.H., Chandraker, M.: Learning to adapt structured output space for semantic segmentation. In: Proceedings of the IEEE conference on computer vision and pattern recognition. pp. 7472–7481 (2018)
  54. Tzeng, E., Hoffman, J., Saenko, K., Darrell, T.: Adversarial discriminative domain adaptation. In: Proceedings of the IEEE conference on computer vision and pattern recognition. pp. 7167–7176 (2017)
  55. Vaswani, A., Shazeer, N., Parmar, N., Uszkoreit, J., Jones, L., Gomez, A.N., Kaiser, L., Polosukhin, I.: Attention is all you need. In: Advances in neural information processing systems. pp. 5998–6008 (2017)
  56. Vu, T.H., Jain, H., Bucher, M., Cord, M., Pérez, P.: Advent: Adversarial entropy minimization for domain adaptation in semantic segmentation. In: Proceedings of the IEEE/CVF Conference on Computer Vision and Pattern Recognition. pp. 2517–2526 (2019)
  57. Wang, D., Shang, Y.: A new active labeling method for deep learning. In: 2014 International joint conference on neural networks (IJCNN). pp. 112–119. IEEE (2014)
  58. Wang, D., Shelhamer, E., Liu, S., Olshausen, B., Darrell, T.: Tent: Fully test-time adaptation by entropy minimization. arXiv preprint arXiv:2006.10726 (2020)
  59. Wang, Z., Wei, Y., Feris, R., Xiong, J., Hwu, W.M., Huang, T.S., Shi, H.: Alleviating semantic-level shift: A semi-supervised domain adaptation method for semantic segmentation. In: Proceedings of the IEEE/CVF Conference on Computer Vision and Pattern Recognition Workshops. pp. 936–937 (2020)
  60. Woo, S., Park, J., Lee, J.Y., Kweon, I.S.: Cbam: Convolutional block attention module. In: Proceedings of the European conference on computer vision (ECCV). pp. 3–19 (2018)
  61. Xia, H., Zhao, H., Ding, Z.: Adaptive adversarial network for source-free domain adaptation. In: Proceedings of the IEEE/CVF International Conference on Computer Vision. pp. 9010–9019 (2021)
  62. Yang, X., Yumer, E., Asente, P., Kralej, M., Kifer, D., Lee Giles, C.: Learning to extract semantic structure from documents using multimodal fully convolutional neural networks. In: Proceedings of the IEEE Conference on Computer Vision and Pattern Recognition. pp. 5315–5324 (2017)

63. Yu, Z., Yu, J., Cui, Y., Tao, D., Tian, Q.: Deep modular co-attention networks for visual question answering. In: Proceedings of the IEEE/CVF Conference on Computer Vision and Pattern Recognition. pp. 6281–6290 (2019)
64. Zhang, H., Goodfellow, I., Metaxas, D., Odena, A.: Self-attention generative adversarial networks. In: International conference on machine learning. pp. 7354–7363. PMLR (2019)
65. Zhdanov, F.: Diverse mini-batch active learning. arXiv preprint arXiv:1901.05954 (2019)
66. Zhong, X., Tang, J., Yepes, A.J.: Publaynet: largest dataset ever for document layout analysis. In: 2019 International Conference on Document Analysis and Recognition (ICDAR). pp. 1015–1022. IEEE (2019)
67. Zhou, F., Shui, C., Yang, S., Huang, B., Wang, B., Chaib-draa, B.: Discriminative active learning for domain adaptation. Knowledge-Based Systems **222**, 106986 (2021)